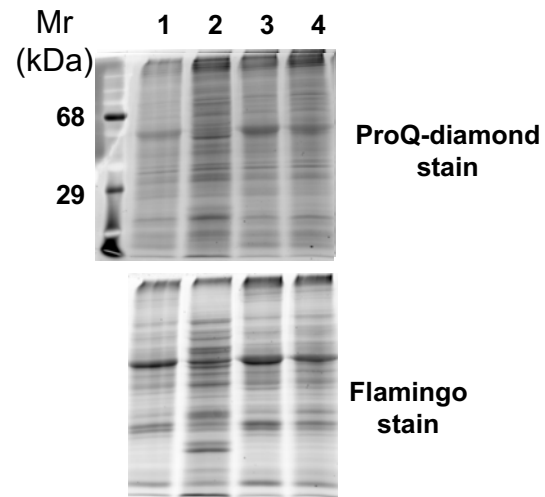


Supplemental Figure 1. cNME-inhibition does not modify the phosphoproteome or protein oxidation levels.

A, A representative SDS-PAGE gel showing the time course of protein phosphorylation in crude homogenates detected with ProQ-diamond staining (top gel). Lanes 1 and 3 correspond to WT plants at 3 and 8 days after germination, respectively. Lanes 2 and 4 correspond to *map1A* mutants treated with 100 nM of Fumagillin for 3 and 8 days after germination, respectively. For normalization, the total amount of protein loaded was determined by staining the gel with Flamingo stain (bottom gel).

B, A representative immunoblot showing the time course of protein carbonylation in crude homogenates, as determined with the Oxiblot Kit. Lanes 1 and 3 refers to WT plants at 3 and 8 days after germination, respectively. Lanes 2 and 4 correspond to *map1A* mutants treated with 100 nM of Fumagillin for 3 and 8 days after germination, respectively. Lanes 5,6,7,8 correspond to negative controls consisting of the same samples shown in lanes 1,2,3,4 not subjected to the derivatization reaction.

A



B

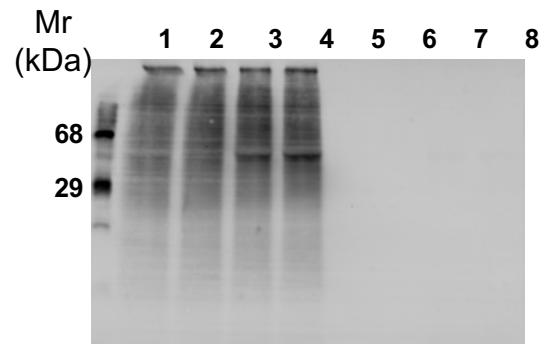


Figure 1

Supplemental Figure 2. Rescue of the defect associated with cNME inhibition in dsRNA interference *Arabidopsis* lines with Cys and impact of iron cations on growth.

A, Plantlets were vertically grown in the presence or absence of 2 mM cysteine. The *ΨMAP1A2* line, a dsRNA-interference *Arabidopsis* line with reduced levels of both MAP1A and MAP2s, mimics the phenotype of the *map1A* line when grown in the presence of 100 nM of Fumagillin. Both the phenotype and MAP content are described in Ross et al. (2005).

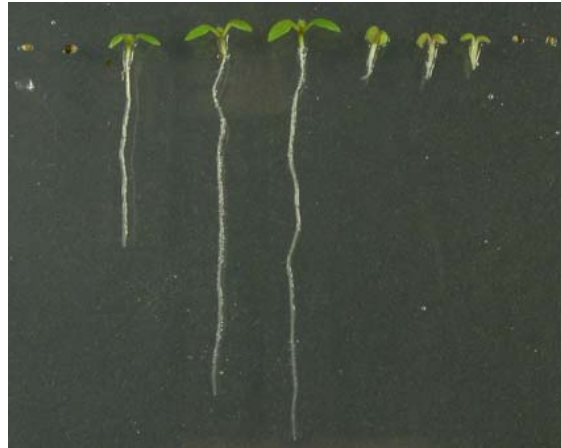
B, *map1A* and WT plantlets were vertically grown in the presence or absence of iron chloride salts (FeII or FeIII) and in the presence or absence of 100 nM Fumagillin. The highest iron concentrations are expected to induce a Fenton reaction producing OH radicals and oxidative stress. The data show that the cNME inhibited line does not exhibit additional oxidative stress sensitivity or protection compared to the controls.

A

ΨMAP1A2
Cys (mM)
- 2mM

**B**

Fumagillin- - - - + + + + +
Fe II (μM) 2000 1000 500 50 - - 50 500 1000 2000

map1A

Fumagillin - - - - + + + + +
Fe II (μM) 2000 1000 500 50 - - 50 500 1000 2000

WT

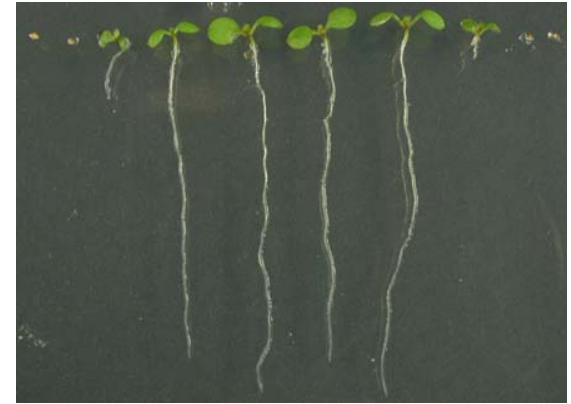


Fumagillin - - - - - + + + +
Fe III (μM) 2000 1000 500 50 - - 50 500 1000 2000

map1A

Fumagillin - - - - - + + + +
Fe III (μM) 2000 1000 500 50 - - 50 500 1000 2000

WT

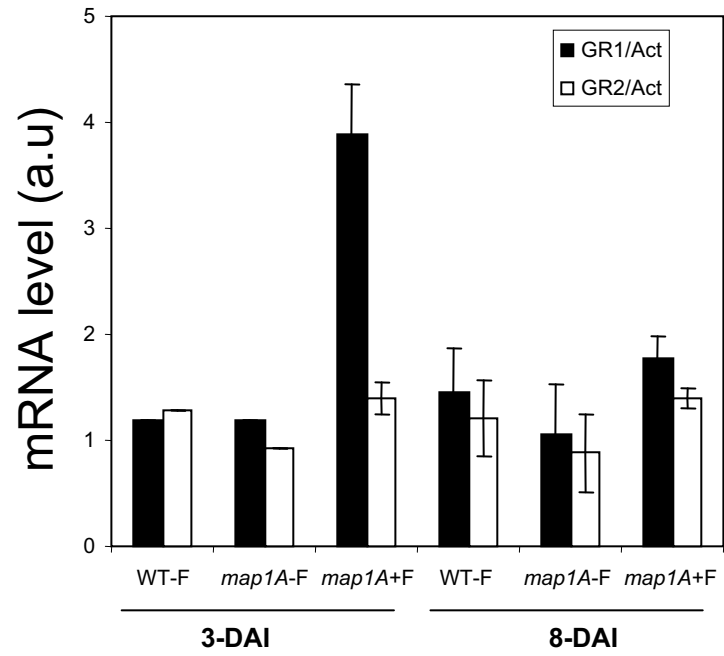
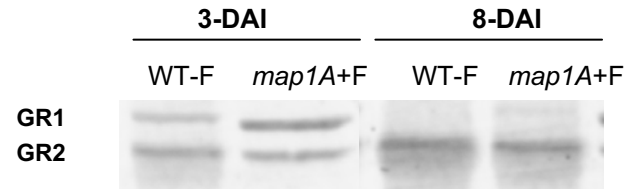
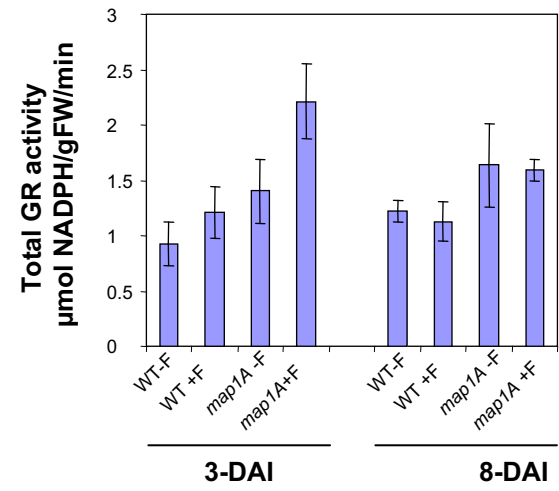
**Figure 2**

Supplemental Figure 3. The high level of GSSG in cNME deficient plants is not due to a decrease in Glutathione reductase concentration.

A, Levels of transcripts for cytoplasmic Glutathione reductase (*GR1*) and chloroplastic Glutathione reductase (*GR2*) expressed relative to actin transcript levels. Measurements were made by real-time PCR. A.u, Arbitrary units.

B, Relative levels of GR1 and GR2 proteins as analyzed by Western blot. We analyzed 30 µg of total proteins by 10% denaturing PAGE, followed by electroblotting and probing of the resulting membrane with an anti-GR antibody recognizing both GR1 and GR2 (Agrisera, Vännäs, Sweden).

C, The total GR activity of the indicated protein extracts was determined as described.

A**B****C****Figure 3**

Supplemental Figure 4. cNME-inhibition rapidly induces a decrease in NADPH nucleotide levels.

The amount of pyridine nucleotides in total extracts from WT and cNME-deficient plants was determined at various stages, as reported in Methods. The measurements of NADH (top, left), NADP (bottom, left) and NADPH (right panel) are displayed.

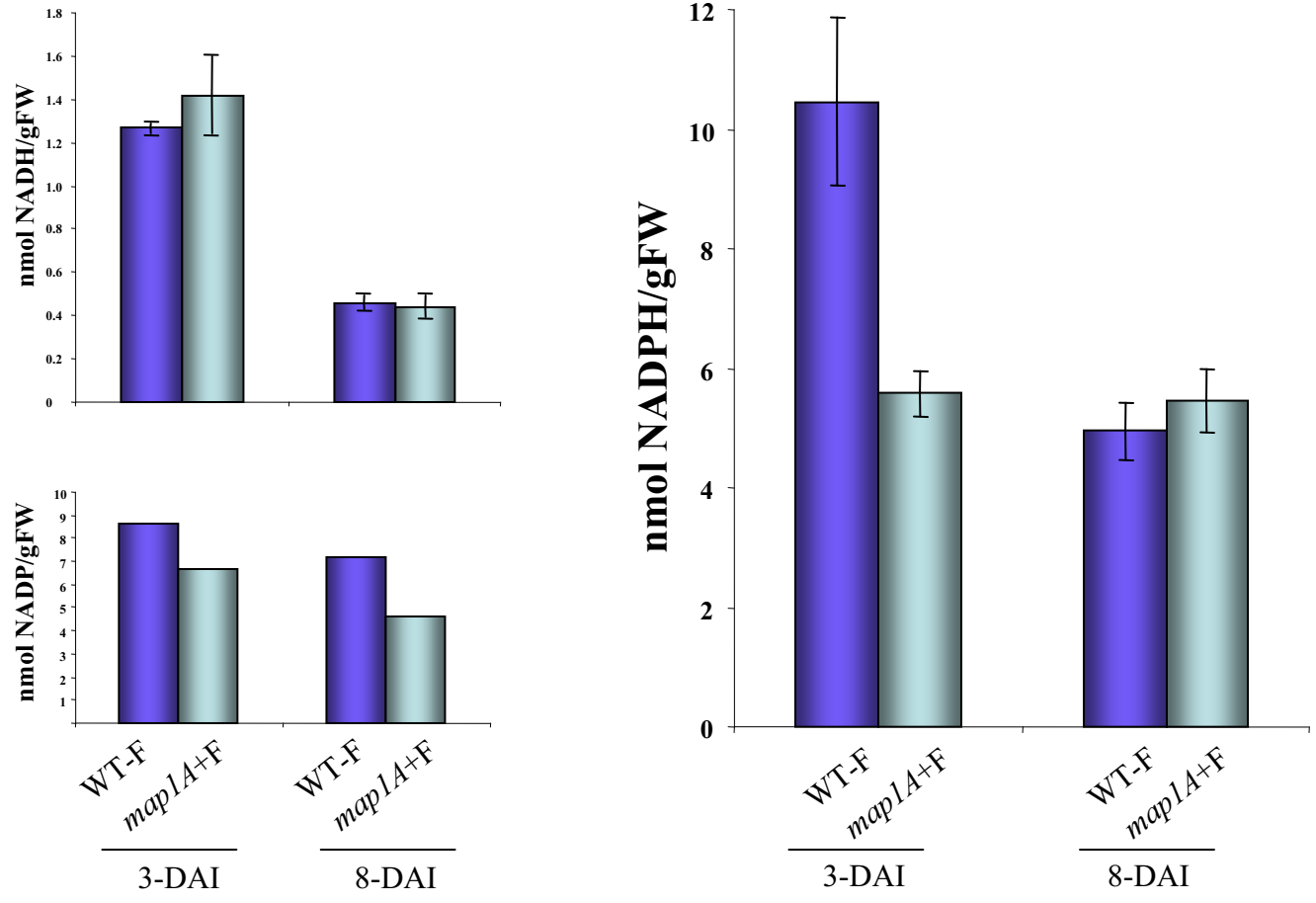


Figure 4

Supplemental Figure 5. NME perturbation induced a slight adjustment of proteolytic activities.

A, Investigation of global proteolytic activities in the sample. 3 and 8-DAI-old seedlings were vertically grown in the presence or absence of 100 nM of Fumagillin. Endoproteolytic activities were measured with the EnzChek peptidase/protease substrate as described in Methods. Mean of activities are given in RFU/min/ μ g of proteins.

B, Late induction of proteasome-like activities following cNME inhibition. Caspase-like, Trypsin-like and Chymotrypsin-like activities were investigated with specific substrates (see Methods for further details) in WT-F and *map1A*+F plantlets at 3 and 8-DAI. Mean specific proteolytic activities (pmol/min/ μ g of protein) are given. P, error probability (two-tailed t-test. Relative Fluorescence Unit, RFU. One star indicates a P value less than 0.05 while two stars indicate a P value less than 0.01.

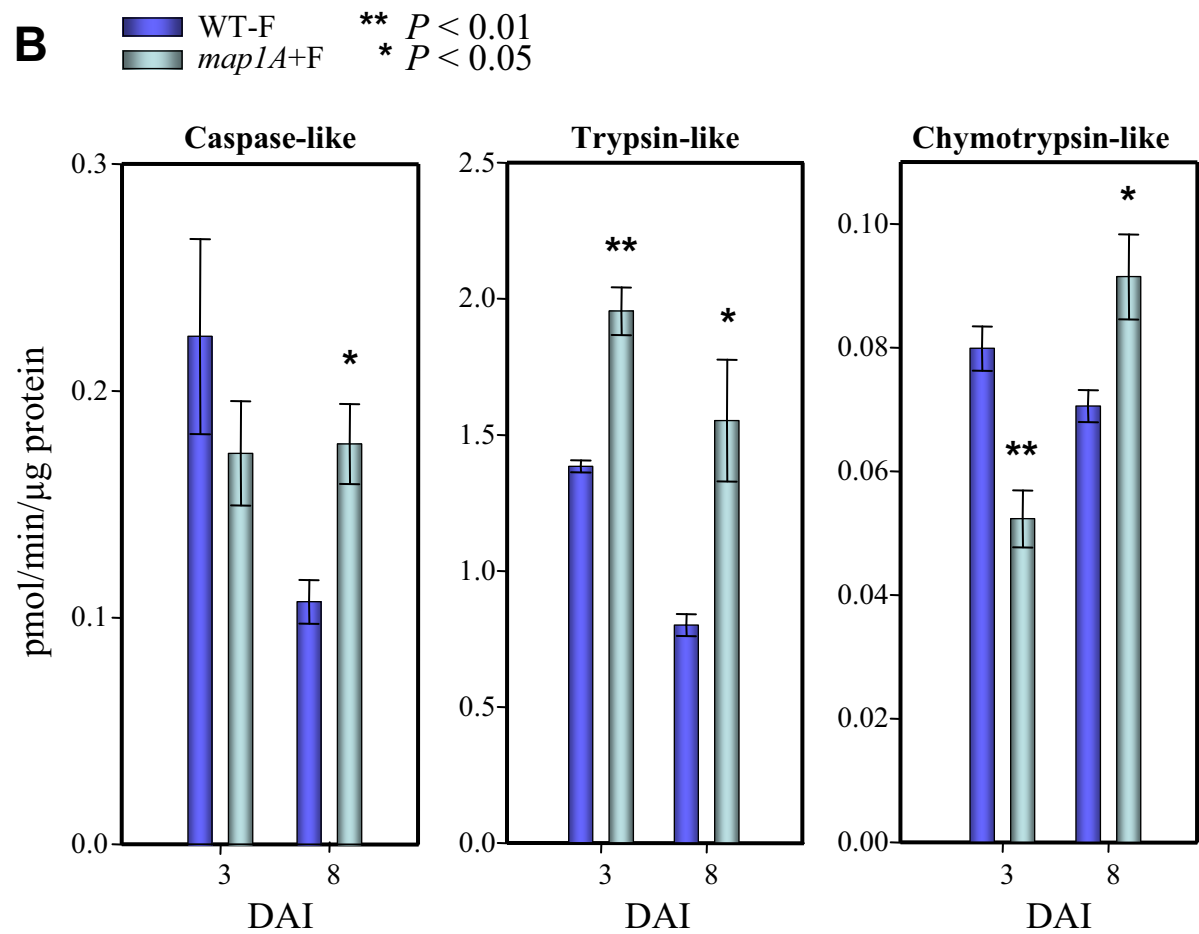
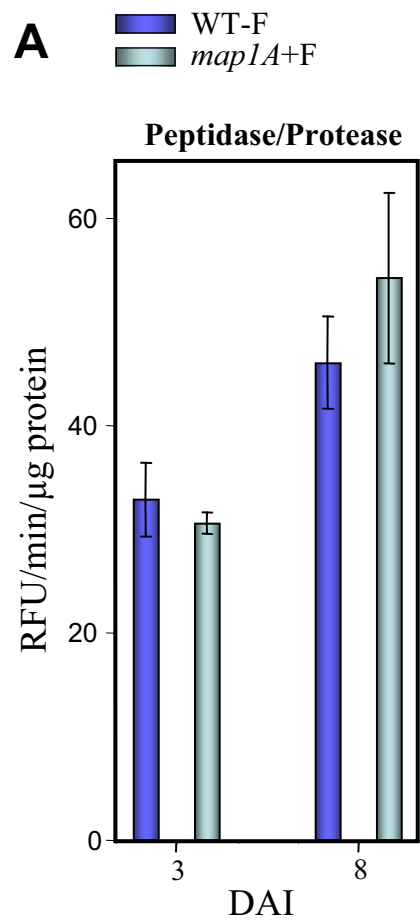


Figure 5

Supplemental Table 1 Identities of protein spots with a higher intensity in NME-inhibited conditions

Spot number	Function	Localization	N-terminus	Measured MW (kDa)	Theoretical MW (kDa)	Measured pI	Theoretical pI
190-212-213 (238 in WT)	AT5G17920 Cobalamine-independent methionine synthase 3	cytoplasmic	ma	67	84	6.6	6.1
190	AT3G03780 Cobalamine-independent methionine synthase 2	cytoplasmic	ma	67	84	6.6	6.1
55	AT1g21720 PBC1 (20S proteasome beta subunit C1)	cytoplasmic	ma	30	23	5.5	5.3
55	AT2g40600 (appr-1-p processing enzyme family protein)	chloroplast	mr	30	21	5.5	5.6
55	AT5G66550 Maf family protein	cytoplasmic	mt	30	20	5.5	4.8
95-96	AT1G53240 malate dehydrogenases (MDH)	glycosomal/mitochondria	mf	38	33	6.4	6.4
75	AT5G23140 CLPP2 (Clp protease proteolytic subunit 2)	chloroplast/mitochondria	mm	31	24	6.4	5.8
222-223	AT1G30230 elongation factor 1-beta	cytoplasm	ma	41	25	4.5	4.4
222	AT2G18110 elongation factor 1-beta, putative	cytoplasm	ma	41	25	4.6	4.5
78	AT4G02520 Glutathione S-transferase PM24	cytoplasm	ma	31	24	6.3	5.9
79	AT1G02930 ATGSTF6 (early responsive to dehydration 11)	cytoplasm	ma	30	23	6.3	5.8

The intensity of the spots in sample *map1A*+F was compared to that of the WT-F sample at 8 DAI.

Supplemental Table 2 Low molecular weight proteins are more abundant in *map1A*+F 3

DAI than in the equivalent fractions from WT.

Spot number	gene	Measured Mr (kDa)	Theoretical Mr (kDa)
1	AT1G62290.1	6.5	60
1	AT5G42890.1	6.5	14
2	AT5G19090.1	6	60
2	AT4G04460.1	6	55
2	AT1G11910.1	6	55
2	AT5G44120.1	6	53
2	AT2G39730.1	6	52
2	AT1G03880.1	6	51
2	AT3G08580.1	6	41
2	AT5G19760.1	6	32
2	AT5G13430.1	6	30
2	AT5G07190.1	6	23
2	AT5G38410.1	6	20
2	AT4G27150.1	6	19
2	AT4G01150.1	6	18
2	AT2G36170.1	6	15
2	AT3G47650.1	6	15
2	AT5G63030.1	6	14
2	AT4G16500.1	6	13
2	AT2G35605.1	6	12
2	AT2G38530.1	6	12
2	AT5G40370.1	6	12
2	AT1G66240.1	6	11
2	AT1G31812.1	6	10
2	AT3G48140.1	6	10
2	AT5G47930.1	6	9
2	AT1G61570.1	6	9
2	AT2G45710.1	6	9
2	AT3G52730.1	6	8
2	AT1G51650.1	6	8
3	AT4G28520.1	4.5	58
4	AT4G28520.1	6.5	58
4	AT1G62290.1	6.5	56
4	AT5G44120.2	6.5	53
4	AT1G03880.1	6.5	51
4	AT1G13440.1	6.5	37
4	AT1G50900.1	6.5	19
4	AT4G01150.1	6.5	18
4	AT1G23410.1	6.5	18
4	AT1G54630.1	6.5	15
4	AT1G54580.1	6.5	15
4	AT4G16500.1	6.5	13
4	AT2G38530.1	6.5	12

4	AT5G40370.1	6.5	12
4	AT1G66240.1	6.5	11
4	AT1G31812.1	6.5	10
4	AT5G47930.1	6.5	9
4	ATCG00580.1	6.5	9
4	AT2G45710.1	6.5	9